MR Assessment of Multi-Modal Targeted Contrast Agent

T. Larson[1], D. Webb[2], K. V. Sokolov[1], and J. A. Bankson[2]

[1]Department of Biomedical Engineering, The University of Texas, Austin, TX, United States, [2]Department of Imaging Physics, The University of Texas M.D. Anderson Cancer Center, Houston, TX, United States

Introduction

Contrast agents that are detectable across multiple imaging modalities improve our diagnostic potential by allowing investigators to exploit the most beneficial and complimentary characteristics of all modalities in order to address a given problem. Contrast agents that are both MR- and optically active, for example, can be localized in anatomical and/or functional context by MRI for subsequent observation on a subcellular scale via optical imaging techniques such as reflectance confocal microscopy [1]. Such an agent would need to exhibit high scatter cross section for optical imaging as well as high relaxation enhancement for detectability by MRI. Iron oxide nanoparticles are known to exhibit the latter but are not detectable by optical methods, while gold nanoshells exhibit the former but provide no mechanism for MR relaxation enhancement. Incorporating maghemite into the core of a gold nanoshell provides enhancement in both MR and optical imaging without interfering with the convenient surface chemistry associated with gold nanoparticles, facilitating physiological passivation and the inclusion of targeting or therapeutic moieties. Here we report observable changes in relaxation enhancement during the implementation of these targeted bimodal nanoparticles.

Methods & Materials

Iron oxide nanoparticles and gold-coated iron oxide nanoparticles were synthesized as previously reported [2] to yield particles with iron cores of radius 5 nm and a shell thickness of approximately 20 nm. Neomarker clone 225 antibodies were attached to a bifunctional hydrazide-PEG-thiol linker to facilitate binding to the gold surface. Some nanoparticles were coated only with PEG-thiol as controls. Total iron concentration was measured by mass spectrometry on an Agilent 7500 quadropole ICP-MS after the nanoparticles were dissolved in a 10% HCl/30% H_2SO_4 acid solution. Samples of raw iron cores (IC), gold-coated iron cores (GIC) , PEGylated gold-coated particles (PGIC), and targeted agents (TPGIC) were diluted in water (IC, GIC, TPGIC), PBS (PGIC), and 2% PEG in PBS (PGIC) for MR characterization. These samples were pipetted into 5 mm NMR sample tubes which were then submerged in a 50mL centrifuge tubes, all of which were aligned along B_0 to minimize any influence from susceptibility mismatch. Five concentrations of each were diluted to provide total iron concentration ranging from 1.15 μg/mL to 23 μg/mL.

To verify functionality of the antiobdy, MDA-MB-468 human breast cancer cells were exposed to TPGIC for 30 minutes at room temperature, washed, spun down, and resuspended in a buffered collagen solution. Three phantoms were created, again in 5 mm NMR sample tubes: one with a layer of pure collagen adjacent to labeled cells; one with a layer of collagen adjacent to unlabeled cells; and one with four layers of cells with concentrations ranging from $1.75x10^6$ cells/mL to $2.2x10^5$ cells/mL.

All images were acquired using a 4.7 T Biospec experimental MR system (Bruker Biospin MRI, Billerica, MA, USA). T1, T2, and T2* of each sample was measured for each particle configuration using a spin-echo saturation-recovery (TE = 10.5 ms; TR = 2500 ms, 1500 ms, 1000 ms, 500 ms, and 200 ms), a Carr-Purcell-Meiboom-Gill spin echo train (TE = 15ms to 360ms in 15ms increments; TR = 1100 ms), and a multi-echo gradient-echo sequence (TE = 1.5 ms to 50.25ms in 3.25 ms increments; TR = 500 ms), respectively. All images were acquired over identical geometries (FOV 32mm x 32 mm; 1 mm slice; 64 x 64 matrix). Images were analyzed using ParaVision® 3.0.2 and rate constants were fit to the Solomon-Bloemberg-Morgan model for relaxation [3,4] using Matlab (The Mathworks, Natick, MA, USA).

Results & Discussion

Gold-coated iron nanoshells enhance contrast between gel samples prepared with and without labeled cells, and between gel samples containing various concentrations of labeled cells as illustrated in Figure 1. Very little spin-lattice relaxation enhancement was observed for any of these samples. Significant spin-spin relaxation enhancement (both r_2 and r_2*) was observed, however, enhancement was reduced upon PEGylation. Figure 2 illustrates this trend for r_2* relaxivities measured from several samples.

Acknowledgements:

This work was supported in part by the National Institutes of Health (CA-016672).

References

[1] Sokolov KV, et al. *Dis Markers* **18**(5-6): 269-91, 2002.
[2] Williams SM, et al., *Analyst* **128**(11): 1352-9, 2003.
[3] Bloembergen N, Morgan L. *J Chem Phys* **34**: 842-50, 1961.
[4] Solomon I. *Phys Rev* **99**: 559-65, 1955.

Figure 1: T2-weighted images illustrating contrast enhancement in cell samples using targeted, gold-coated iron nanoparticles. Unlabeled cells in gel (bottom of sample on left) clearly distinguished from labeled cells in gel (bottom of sample on right) and from graded density of labeled cells (center).

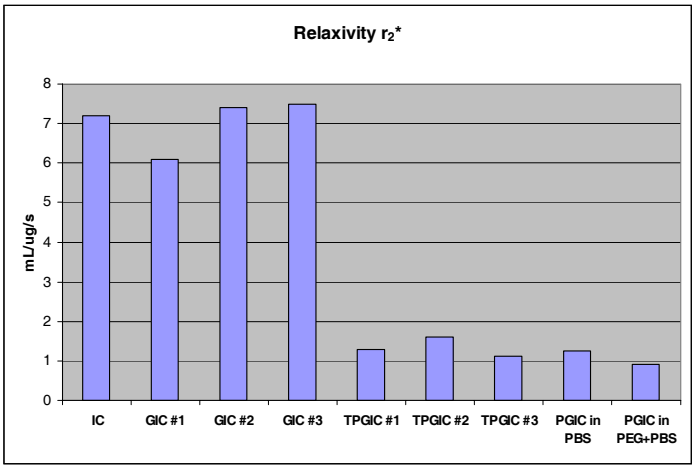

Figure 2: Relaxivities exhibited by particles at various stages of manufacture. Relaxivity is significantly diminished following PEGylation.